AMERICAN SOCIETY FOR MICROBIOLOGY | Antimicrobial Agents and Chemotherapy

# Personalized Therapeutic Cocktail of Wild Environmental Phages Rescues Mice from *Acinetobacter baumannii* Wound Infections

**James M. Regeimbal,[a] Anna C. Jacobs,[b] Brendan W. Corey,[b] Matthew S. Henry,[c] Mitchell G. Thompson,[b]* Rebecca L. Pavlicek,[a]* Javier Quinones,[c] Ryan M. Hannah,[d] Meron Ghebremedhin,[e] Nicole J. Crane,[e] Daniel V. Zurawski,[b] Nimfa C. Teneza-Mora,[a] Biswajit Biswas,[c] Eric R. Hall[a]**

Wound Infections Department, Naval Medical Research Center, Silver Spring, Maryland, USA[a]; Wound Infections Department, Walter Reed Army Institute of Research, Silver Spring, Maryland, USA[b]; Biological Defense Research Directorate, Naval Medical Research Center—Frederick, Fort Detrick, Maryland, USA[c]; National Bioforensic Analysis Center, National Biodefense and Countermeasures Center, Fort Detrick, Maryland, USA[d]; Regenerative Medicine Department, Naval Medical Research Center, Silver Spring, Maryland, USA[e]

**Multidrug-resistant bacterial pathogens are an increasing threat to public health, and lytic bacteriophages have reemerged as a potential therapeutic option. In this work, we isolated and assembled a five-member cocktail of wild phages against *Acinetobacter baumannii* and demonstrated therapeutic efficacy in a mouse full-thickness dorsal infected wound model. The cocktail lowers the bioburden in the wound, prevents the spread of infection and necrosis to surrounding tissue, and decreases infection-associated morbidity. Interestingly, this effective cocktail is composed of four phages that do not kill the parent strain of the infection and one phage that simply delays bacterial growth *in vitro* via a strong but incomplete selection event. The cocktail here appears to function in a combinatorial manner, as one constituent phage targets capsulated *A. baumannii* bacteria and selects for loss of receptor, shifting the population to an uncapsulated state that is then sensitized to the remaining four phages in the cocktail. Additionally, capsule is a known virulence factor for *A. baumannii*, and we demonstrated that the emergent uncapsulated bacteria are avirulent in a *Galleria mellonella* model. These results highlight the importance of anticipating population changes during phage therapy and designing intelligent cocktails to control emergent strains, as well as the benefits of using phages that target virulence factors. Because of the efficacy of this cocktail isolated from a limited environmental pool, we have established a pipeline for developing new phage therapeutics against additional clinically relevant multidrug-resistant pathogens by using environmental phages sourced from around the globe.**

The increasing prevalence of multidrug resistant (MDR) bacterial pathogens is a major public health threat. Of particular concern are the ESKAPE pathogens (*Enterococcus faecium*, *Staphylococcus aureus*, *Klebsiella pneumoniae*, *Acinetobacter baumannii*, *Pseudomonas aeruginosa*, and *Enterobacter* spp.), which are often nosocomial in nature and can cause severe local and systemic infections (1, 2). Among the ESKAPE pathogens, *A. baumannii* is a Gram-negative, capsulated, opportunistic pathogen that is easily spread in hospital intensive care units (ICU) (3). Many *A. baumannii* clinical isolates are also MDR, which severely restricts the available treatment options, with untreatable infections in traumatic wounds often resulting in prolonged healing times, the need for extensive surgical debridement, and in some cases the further or complete amputation of limbs (4–14). Thus, there is an urgent need for new therapeutics against the MDR ESKAPE pathogens, including *A. baumannii*.

One possible therapeutic against ESKAPE pathogens is bacteriophages (phages). Phages are diverse viruses that replicate within and can kill specific bacterial hosts. The possibility of harnessing lytic phages as an antibacterial was investigated following their initial isolation (15). However, phage therapy was largely abandoned in the United States by 1934 following the discovery of penicillin, and only recently has interest in phage therapeutics been renewed (16–27).

Phages are universally abundant in the environment, making the isolation of potentially therapeutic phages from sources such as untreated sewage water very straightforward (20, 22, 28). The primary factors affecting the successful isolation of such phages are the availability of a robust collection of clinically relevant bacterial pathogens to serve as hosts and access to diverse environmental sampling sites. With these conditions met, simple screening methods can be employed to rapidly isolate and amplify lytic phages specific to a bacterial pathogen(s) of interest, and their therapeutic potential can be investigated (20, 22, 23, 26–28).

The host range of a given phage is often very specific to the subspecies level, which may confer an advantage over antibiotics if infectious bacteria can be targeted without damaging commensal

**Received** 2 December 2015 **Returned for modification** 6 January 2016
**Accepted** 6 July 2016

**Accepted manuscript posted online** 18 July 2016

**Citation** Regeimbal JM, Jacobs AC, Corey BW, Henry MS, Thompson MG, Pavlicek RL, Quinones J, Hannah RM, Ghebremedhin M, Crane NJ, Zurawski DV, Teneza-Mora NC, Biswas B, Hall ER. 2016. Personalized therapeutic cocktail of wild environmental phages rescues mice from *Acinetobacter baumannii* wound infections. Antimicrob Agents Chemother 60:5806–5816. doi:10.1128/AAC.02877-15.

Address correspondence to Biswajit Biswas, biswas.biswajit.ctr@mail.mil.

* Present address: Mitchell G. Thompson, University of California Berkeley, Berkeley, California, USA; Rebecca L. Pavlicek, NAMRU-Asia, Singapore.

J.M.R. and A.C.J. contributed equally to this report.

Supplemental material for this article may be found at http://dx.doi.org/10.1128/AAC.02877-15.

members of the host microbial community. However, because of the specificity of the phage, viable phage therapeutics will also likely require a significant level of personalization, as each phage targets its host via a specific receptor on the bacterial surface. Resistance to a phage can also occur if the receptor mutates or is lost, and thus it is advantageous to procure multiple phages against a pathogen, each with as broad and as distinct a host range for strains of the targeted pathogen as possible. Combining such phages into a single treatment cocktail may extend the utility of a personalized cocktail and reduce the frequency of phage cocktail resistance and therapeutic failure (23).

In this work, we isolated lytic phages specific to *A. baumannii* from limited environmental sources and compounded a proof-of-concept five-member phage cocktail against the model MDR pathogen *A. baumannii* AB5075 (29). Further, we successfully demonstrated the efficacy of this cocktail in a murine full-thickness wound infection model. These results highlight the potential for developing targeted phage therapeutics to combat the growing threat of MDR bacterial pathogens.

## MATERIALS AND METHODS

**Bacterial strains and culture conditions.** Two strains were used to isolate phages in this study. *A. baumannii* AB5075 is a previously described clinical strain that was isolated at Walter Reed Army Medical Center (29). AB5075Passaged (AB5075P) was isolated after passage of AB5075 in our mouse wound model for 14 days (30). The reisolated AB5075 showed mixed colony morphology on Lennox LB agar (Becton, Dickinson and Company, Sparks, MD) of opaque (wild-type) and translucent colonies. A colony that displayed translucent morphology was chosen as a second target strain for phage isolation and designated AB5075P. In order to visualize wound bacterial burden during animal studies, the bioluminescent strain AB5075 *att*Tn*7*::*luxCDABE* (AB5075::lux) was created. Briefly, a Tn*7* plasmid containing the *lux* operon *luxCDABE*, pUC18T-mini-Tn*7*T-hph-lux, was introduced into AB5075 via conjugation (31), and integration of the *lux* operon into the chromosome at the *att*Tn*7* site was confirmed via PCR. Additionally, two Tn*5* isogenic AB5075 mutants, AB5075 *epsA*::Tn*5* and AB5075 *ptk*::Tn*5*, were used in several *in vitro* assays (29). *A. baumannii* strains used to assess differences in host infectivity of phages AB-Navy1 to AB-Navy4 (AB-Navy1–4) are genetically diverse strains that were obtained from our Wound Infections culture collection and were originally received via the Army Multidrug-Resistant Organism Repository and Surveillance Network (MRSN) and the Navy NAMRU-6. MDR *A. baumannii* clinical isolates used to assess phage cocktail specificity are military-relevant clinical isolates from wounded service members and were isolated from Landstuhl Regional Medical Center, National Navy Medical Center, and Walter Reed National Military Medical Center between 2003 and 2010 during the height of the conflicts in Afghanistan and Iraq (R. Heitkamp, A. Zale, and B. Kirkup, submitted for publication). Strains were maintained on tryptic soy broth (TSB; Becton, Dickinson and Company) or Lennox LB broth (Becton, Dickinson and Company) and stored in 20 to 40% glycerol at −80°C.

**Isolation of phage strains from environmental sources.** *A. baumannii* phages were isolated from raw sewage water harvested from the Seneca Wastewater Treatment Plant located in Germantown, Maryland. Briefly, powdered TSB medium (Becton, Dickinson and Company) was mixed with raw sewage to a final concentration of 3% (wt/vol). AB5075 or AB5075P was grown to exponential phase, and 1 ml of each strain was added to 100-ml aliquots of the TSB-sewage mixture. The *A. baumannii*-inoculated TSB-sewage mixture was incubated at 37°C and 250 rpm overnight. The following day, 1 ml of the infected TSB-sewage mixture was harvested and centrifuged at 8,000 × *g* for 5 min to pellet cells and debris. The supernatant was transferred to a sterile 0.22-μm Spin-X centrifuge tube filter (Corning, NY) and centrifuged at 6,000 × *g* to remove any remaining bacteria. A 10-μl aliquot of the filtrate was mixed with 100 μl of exponential-growth culture of AB5075 or AB5075P, incubated at 37°C for 20 min, mixed with 2.5 ml of molten top agar (0.6% agar) tempered to 50°C, and poured over TSB agar plates (1.5% TSB agar). The plates were incubated overnight at 37°C, and subsequent phage plaques were individually harvested and purified three times on appropriate *A. baumannii* isolates by use of the standard procedures described by Sambrook et al. (28).

**Propagation and purification of phage strains.** High-titer phage stocks for *in vivo* experimentation were propagated and amplified in corresponding host bacteria by standard procedures (20). Large-scale phage preparations were purified by cesium chloride density centrifugation as previously described (22) and filtered through a 0.22-μm filter (Millipore Corporation, Billerica, MA) prior to the treatment of animals. Phage stocks were stored at 4°C indefinitely.

**Electron microscopy.** Standard methods of sample preparation were employed for transmission electron microscopy (TEM) and scanning electron microscopy (SEM). For both methods, samples were fixed in 4% paraformaldehyde with 1% glutaraldehyde in 0.1 M sodium cacodylate buffer. For TEM, the fixed and inactivated high-titer phage samples were spread on a copper grid, washed with water, and negatively stained with uranyl acetate. These samples were imaged in a FEI Tecnai T12 Spirit TEM at 100 kV.

For SEM, fixed Tegaderm dressing samples were washed three times with 0.1 M sodium cacodylate buffer and postfixed with 1% osmium tetroxide in buffer and then 0.5% uranyl acetate in water. The samples were subsequently dehydrated through an ethanol series, critically point dried, and coated with gold-palladium. The coated SEM samples were imaged in an FEI Quanta 200 FEG SEM at 5 kV.

**High-throughput liquid lysis assay to determine host infectivity and cocktail synergy.** An automated, indirect, liquid lysis assay was used to evaluate the activity of phages against *A. baumannii* strains (32). Briefly, an overnight culture of each strain was inoculated into the wells of a 96-well plate containing TSB mixed with 1% (vol/vol) tetrazolium dye. Phages were added to each well, and plates were incubated in an OmniLog system (Biolog, Inc., Hayward, CA) at 37°C overnight. The tetrazolium dye indirectly measures the respiration of the bacterial cells. Respiration causes reduction of the tetrazolium dye, resulting in a color change to purple. The color intensity of each well was quantified as relative units of bacterial growth. For host infectivity determination, bacteria were inoculated at $10^5$ CFU per well and phages were added at a concentration of $10^6$ PFU per well for a multiplicity of infection (MOI) of 10. For cocktail synergy studies, bacteria were inoculated at $10^6$ CFU per well and phages were added at a concentration of $10^8$ PFU per well for an MOI of 100.

**Efficiency of plating for phages on the host strain.** To determine how well each phage infected its original host strain, a dilution series spot plate assay was used to observe plaque formation (28). To do so, 50 μl of an overnight culture of each *A. baumannii* strain was used to individually inoculate 5 ml of molten top agar tempered to 55°C. The inoculated agar was mixed thoroughly by brief vortexing and then spread over square LB agar plates. Top agar was allowed to set for approximately 45 min, at which time 4-μl aliquots of $10^{10}$ to $10^2$ PFU in 10-fold dilutions of each phage were spotted on the surface. Spots were allowed to fully absorb into the top agar, after which plates were incubated at 37°C for 24 h and plaque formation was assessed.

**Time-kill analysis of *A. baumannii* AB5075 treated with phages.** Time-kill experiments were used to provide a quantitative analysis of phage bactericidal activity. Briefly, an overnight culture of AB5075 was diluted 1:1,000 in fresh LB broth to a final concentration of ~$1 \times 10^6$ CFU per ml. Twenty-milliliter aliquots were then transferred to 250-ml Erlenmeyer flasks and incubated at 37°C with shaking at 200 rpm for 2 h. Samples were then challenged with either $2 \times 10^{11}$ PFU per ml of AB-Army1 or an equal volume of sterile phosphate-buffered saline (PBS) and returned to incubation as previously described. One-hundred-microliter aliquots were taken at 0, 2, 4, and 24 h, serially diluted in PBS, and plated

on LB agar. Plates were incubated at 37°C for 24 h, and colonies were subsequently enumerated.

**Raman spectroscopic analysis of *A. baumannii* strains.** Changes in AB5075 strains due to phage exposure were monitored using Raman spectroscopy. Each sample was obtained from LB agar plates and directly transferred into a disposable weigh dish for spectral collection. Raman spectra were collected using an 830-nm Raman PhAT system (Kaiser Optical Systems, Inc., Ann Arbor, MI, USA). Spectra were collected using a 3-mm spot size lens with 100 s of total acquisition time and a 1-mm spot size lens with 100 s of total acquisition time for time-kill assay samples. Spectra were then preprocessed by baseline removal using a sixth-order polynomial and intensity normalization to the 1,445 $cm^{-1}$ Raman vibrational band prior to analysis.

**Assessment of *A. baumannii* virulence in a *Galleria mellonella* worm model.** Colonies of AB5075 bacteria previously exposed to AB-Army1 phages display a translucent phenotype similar to *A. baumannii epsA* and *ptk* capsule mutants known to be attenuated for virulence (33, 34). To determine if AB5075 previously exposed to AB-Army1 phage is attenuated, we assessed bacterial virulence in a wax worm model of infection (35). *A. baumannii* strains were grown to exponential phase, washed in PBS, and resuspended in PBS to ~$1 \times 10^7$ CFU per ml. *Galleria mellonella* worms (Vanderhorst, Inc., St. Marys, OH) in the final-instar larval stage and between 200 and 300 mg were inoculated with 5 μl of resuspended bacteria into their last left proleg using a 10-μl Hamilton syringe (Fisher Scientific, Pittsburgh, PA). After infection, worms were incubated in plastic petri dishes at 37°C and monitored for death over 5 days. Worms were considered dead when they displayed no movement in response to tactile stimuli.

**Efficacy of phages as a therapeutic in an *A. baumannii* mouse wound model.** Phage treatment was assessed in a previously described mouse wound model (30), with some modifications. Briefly, 6-week-old female BALB/c mice were rendered neutropenic via cyclophosphamide injection, their backs were shaved, and a full-thickness wound was created on the dorsal side of each mouse. Each wound was inoculated with ~$5 \times 10^4$ CFU of AB5075::lux, and a Tegaderm bandage was placed over the wound. Mice were housed singly from day 0 (inoculation) through day 6. For phage treatments, mice received $4 \times 10^9$ PFU of phages in PBS via an intraperitoneal injection and $5 \times 10^9$ PFU of phages in PBS topically under the Tegaderm dressing, on top of the wound. Treatments were given simultaneously at 4, 24, and 48 h postinfection. On day 3 postinfection, each Tegaderm dressing was removed and the wounds were left exposed to air for the remainder of the experiment. Select Tegaderm dressings were submitted for scanning electron microscopy (SEM) to compare biofilm formations among treatment groups. Mouse weights and clinical scores were monitored and recorded through day 6 of the experiment. An IVIS *in vivo* imaging system (PerkinElmer, Waltham, MA) was used to measure the bioluminescent signal of AB5075::lux as a means to visualize and perform relative quantification of bacterial burdens in the wound beds over the course of the experiment. To do so, mice were anesthetized with isoflurane gas and placed dorsal side up, inside the IVIS chamber. Bioluminescence measurements were taken with exposure times of 1, 5, and 10 s on days 1, 3, and 5, respectively. Using Living Image Software version 4.2 (PerkinElmer), pictures were analyzed and bioluminescence was quantified. To determine the average radiance, each wound was measured using a region of interest (ROI) of 2.8 $cm^2$. The area of bioluminescence was measured using the Auto ROI function with a threshold of 20%. The physical wound size was measured using a Silhouette wound measurement device (Aranz Medical Ltd., Christchurch, New Zealand) on days 3, 7, 9, and 13 postinfection.

Research was conducted in compliance with the Animal Welfare Act and other federal statutes and regulations relating to animals and experiments involving animals and adheres to principles stated in the *Guide for the Care and Use of Laboratory Animals* (36). The study protocol was reviewed and approved by the Walter Reed Army Institute of Research/Naval Medical Research Center Institutional Animal Care and Use Committee in compliance with all applicable Federal regulations governing the protection of animals in research.

## RESULTS

**Characterization of *Acinetobacter baumannii* phages isolated from sewage water.** To develop and test a customized phage therapeutic for the treatment of an MDR *A. baumannii* wound infection, the model clinical isolate AB5075 was selected (29). This MDR *A. baumannii* strain has been used successfully in our murine wound model and causes a severe skin and soft tissue infection in mice (30). *In vitro* cultures of *A. baumannii* AB5075 show mixed opaque and translucent colonies at a ratio of 100:1 (data not shown). Because wound healing is a lengthy process that likely exerts unknown selection pressures on *A. baumannii*, we passaged AB5075 in the aforementioned wound model, and when it was reisolated, we chose a translucent colony to approximate a murine clinical isolate with a rare colony morphology (see Materials and Methods). This passaged strain with a translucent morphology was chosen as a second target for phage isolation and was named AB5075P. Lytic phages were then isolated from local sewage water using AB5075 or AB5075P as a host. From the AB5075 sewage water culture supernatant, one phage was isolated and designated AB-Army1 (Fig. 1A), and it produced clear point plaques (Fig. 1B). Interestingly, immediately surrounding the AB-Army1 plaque, there was a large zone of AB5075 that was phenotypically distinct from AB5075 in the adjacent lawn. Halos of this kind implicate a diffusible phage-encoded protein causing an enzymatic change to the surface of the bacteria, a well-recognized phenomenon of phages that infect capsular bacteria (37–44). An efficiency-of-plating assay showed that when a dilution series from $10^{10}$ to $10^2$ of AB-Army1 was spotted on an overlay plate of AB5075, AB-Army1 could infect at a concentration as low as $10^2$ PFU per ml. From AB5075P sewage water culture supernatants, four unique phages were isolated and designated AB-Navy1–4. All four phages displayed gross morphologies similar to each other but much larger than that of AB-Army1 (Fig. 1A) and produced clear point plaques (Fig. 1B). An efficiency-of-plating assay showed that when a dilution series of $10^{10}$ to $10^2$ of all four individual phages was spotted on an overlay plate of AB5075P, all four phages could infect at a concentration as low as $10^3$ PFU per ml. To demonstrate that phages AB-Navy1–4 were each unique, each was tested against a genetically diverse set of *A. baumannii* strains to compare host ranges by use of a Biolog system (32). The host range of each phage was distinct, not only when the strains infected were compared but also when the numbers of hours each phage could prevent growth of the bacterial host in liquid (hold time) were compared (Table 1). Thus, each of these phages to AB5075P appears to be unique.

**AB-Army1 infection leads to a putative loss-of-capsule phenotype in *A. baumannii* AB5075.** The infection of AB5075 with AB-Army1 was monitored in liquid cultures via a time-kill assay. In the absence of AB-Army1, AB5075 grows well, with a largely uniform opaque colony morphology indicative of capsule production. However, when AB-Army1 was present, there was a 3-log reduction in the number of CFU at the 2-h time point compared to that of the uninfected culture (Table 2). Additionally, 98% of the surviving AB5075 bacteria in the AB-Army1-infected culture now had a translucent colony morphology at 2 h, suggesting a loss of capsule production. It should be noted that phages were not inactivated or removed from the culture before plating, so phage

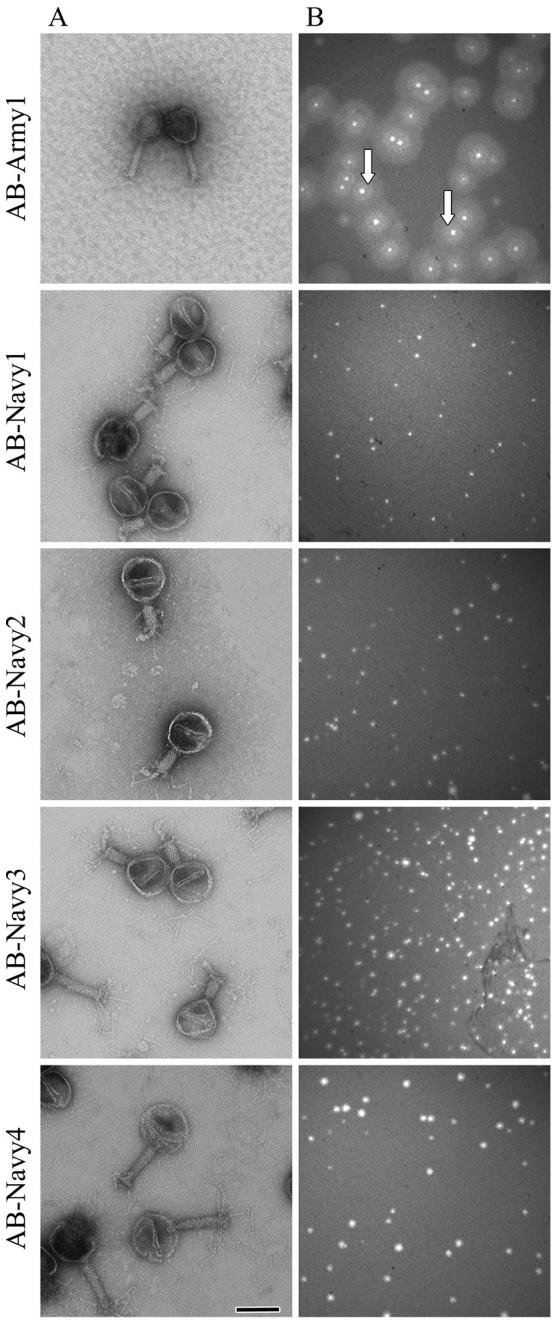


**FIG 1** (A) Electron micrographs of AB-Army1 and AB-Navy1–4. Scale bar, 100 nm. (B) Plaque morphologies of AB-Army1 and each of the AB-Navy1–4 phages on AB5075 and AB5075P LB top agar plates, respectively.

**TABLE 2** AB-Army1 phage infection leads to a putative loss-of-capsule phenotype in *A. baumannii* AB5075

| Time of infection (h) | Treatment | % of capsule-positive bacteria | % of capsule-negative bacteria | Total no. of CFU |
|---|---|---|---|---|
| 0 | Untreated | 100 | 0 | 8.9E + 06 |
| | AB-Army1 | 99 | 1 | 8.2E + 06 |
| 2 | Untreated | 98 | 2 | 2.2E + 09 |
| | AB-Army1 | 2 | 98 | 3.5E + 06 |
| 4 | Untreated | 93 | 7 | 1.7E + 10 |
| | AB-Army1 | 3 | 97 | 6.1E + 08 |
| 24 | Untreated | 85 | 15 | 1.3E + 11 |
| | AB-Army1 | 1 | 99 | 3.5E + 11 |

infection and lysis might have occurred in liquid and/or on the agar plate; however, lysis occurring under either circumstance would result in the same outcome observed here. In contrast, the uninfected AB5075 culture showed a frequency of only 2% translucent colonies at 2 h (Table 2). The surviving translucent AB5075 bacteria in the AB-Army1-infected culture then grew over time, as indicated by the increase in number of CFU (titer) at the 4- and 24-h time points (Table 2). This observed translucent morphology of AB5075 bacteria previously exposed to AB-Army1 is stable for at least 10 restreaks and does not appear to be the transient phase variation observed by Tipton et al. (45). Because the AB-Army1-treated culture still contained phages and grew at 4 and 24 h, we hypothesized that the translucent morphology of the surviving AB5075 bacteria was associated with an insensitivity to the AB-Army1 phage. This phenomenon is consistent with selection for the loss of receptor and suggests that the receptor for AB-Army1 is a capsule component.

When further investigated, it was confirmed that the translucent colony morphology observed in AB5075 previously exposed to AB-Army1 was similar to the colony morphology of isogenic AB5075 mutants harboring Tn*5* insertions in genes known to be involved in capsule biosynthesis. The genes *epsA* and *ptk*, encoding a putative polysaccharide export protein and a protein tyrosine kinase, respectively, are essential for capsule biosynthesis in *A. baumannii* (33, 34, 46). Notably, the translucent colony morphology was also similar to the translucent phenotype of AB5075P, the strain used to isolate phages AB-Navy1–4. When the host ranges of AB-Army1 and the AB-Navy1–4 phages were assessed against the capsule-positive AB5075 and the capsule-negative AB5075P, AB5075 *epsA*::Tn*5*, AB5075 *ptk*::Tn*5*, and a streak-purified strain of AB5075 previously exposed to the AB-Army1 phage, AB-Army1 could form plaques only on capsule-positive AB5075 bacteria, while the AB-Navy1–4 phages could form

**TABLE 1** Host ranges of phages AB-Navy1–4 tested against a genetically diverse set of *A. baumannii* strains

| | Host infectivity of indicated strain[a] | | | | | | | |
|---|---|---|---|---|---|---|---|---|
| Phage | N0326 | P0360 | Q0683 | Q0668 | W0053 | W4448 | W4932 | W5256 |
| AB-Navy1 | 48 | DNI | DNI | 4 | 20 | DNI | 48 | DNI |
| AB-Navy2 | 48 | DNI | DNI | DNI | 18 | DNI | 20 | 36 |
| AB-Navy3 | 48 | 12 | 6 | 6 | 22 | 16 | 48 | 38 |
| AB-Navy4 | 12 | 16 | 22 | DNI | 24 | 12 | 38 | DNI |

[a] Host infectivity is given in hours of hold time (i.e., time that the phage could prevent bacterial growth in liquid). DNI, does not infect.

plaques only on the capsule-negative strains. Thus, it appears that exposure of AB5075 to AB-Army1 not only has a strong bactericidal effect but also imposes a selection that results in a population of insensitive bacteria displaying a phenotype consistent with loss of capsule production by AB5075.

**Raman spectroscopy links capsule changes among phage-treated and untreated AB5075 strains to specific spectral features.** As a biophysical means to rapidly characterize the capsule-associated phenotypes we observed in our studies, Raman spectroscopy was used to interrogate changes in our *A. baumannii* strains. Analysis of Raman spectra revealed inherent spectral markers for capsulated AB5075 strains (Fig. 2). Specifically, the Raman spectral band at 979 $cm^{-1}$ was present only in strains with an opaque, capsule-positive colony morphology. The Raman spectral band at 979 $cm^{-1}$ was absent in the remaining strains, which have a capsule-negative colony morphology (Fig. 2A). Other spectral markers observed in the opaque strain of AB5075 included 1,422 $cm^{-1}$ and 1,379 $cm^{-1}$ (Fig. 2B). While it is difficult to say precisely which cellular components in the bacteria the Raman spectral differences are attributed to, the distinct differences between wild-type AB5075 and the translucent strains, particularly AB5075 *epsA*::Tn*5* and AB5075 *ptk*::Tn*5*, clearly correlate changes in the 979 $cm^{-1}$ band with the changes in capsule phenotype. Raman spectral bands between 1,300 $cm^{-1}$ and 1,480 $cm^{-1}$ are largely attributed to $CH_2$ deformation and scissoring modes present in fatty acids (lipids) and molecules with long chains of methyl and methylene groups (proteins), known components of the bacterial cell surface (47, 48). The structure of the capsular polysaccharide in AB5075 has also recently been proposed and implicates the *epsA* and *ptk* loci for capsular polysaccharide biosynthesis specifically in AB5075 (46).

**Infection of *A. baumannii* AB5075 with phages AB-Army1 and AB-Navy1–4 leads to effective killing *in vitro*.** The results described above revealed that when AB5075 is exposed to AB-Army1, a selection for loss of receptor (capsule) occurs, resulting in a population of translucent colonies that are now sensitive to the AB-Navy1–4 phages. We hypothesized that the combination of all five phages into a single cocktail could result in a robust treatment that targets not only the original opaque AB5075 population but also the emergent and capsule-negative AB-Army1-insensitive bacteria. To test this, a coinfection with the five-member phage cocktail, designated the AB cocktail, was assessed *in vitro* against AB5075 by use of a Biolog system (32). AB5075 cultures treated with only AB-Navy1–4 phages demonstrated growth kinetics similar to that of PBS-treated controls (Fig. 3), further showing that the capsulated AB5075 is insensitive to these phages. The culture containing AB-Army1 showed a 3-h lag in exponential growth, consistent with a selection event against capsulated AB5075 and the following outgrowth of uncapsulated cells in the culture. However, cultures that contained the AB cocktail showed complete growth inhibition over the course of the experiment (Fig. 3). Additionally, Raman spectra collected for each treatment at 0, 4, and 24 h showed that the Biolog results were consistent with the loss of capsule observed in the time-kill experiments. AB5075 cultures that were PBS treated or treated with AB-Navy1–4 phages possessed the 979 $cm^{-1}$ Raman spectral band for all time points, while AB5075 cultures treated with AB-Army1 or the AB cocktail exhibited a greatly diminished 979 $cm^{-1}$ band at 4 and 24 h. Thus, there appears to be a combinatorial effect when all five phages are administered as a single therapeutic cocktail *in vitro*. To further assess the AB cocktail activity, its infectivity against a panel of 92 MDR *A. baumannii* clinical isolates collected between 2003 and 2010 from wounded military personnel being treated at Landstuhl Regional Medical Center, National Navy Medical Center, and Walter Reed National Military Medical Center was tested.

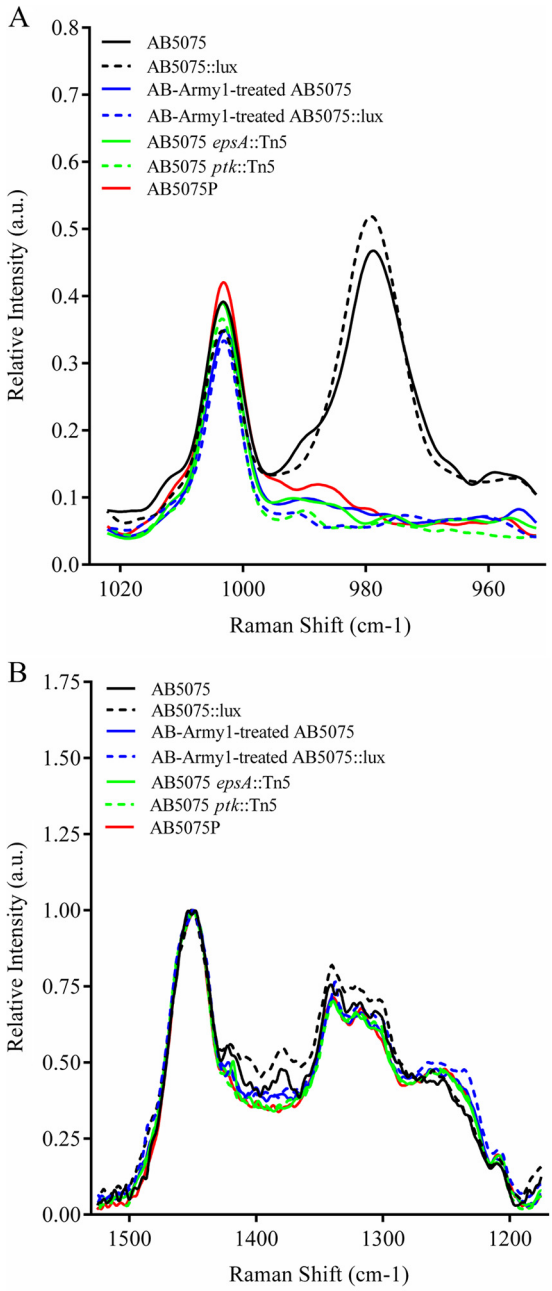


**FIG 2** Raman spectroscopy to characterize the capsule status of *A. baumannii* strains. *A. baumannii* strains were grown in LB medium in the absence or presence of phage, pelleted by centrifugation, and analyzed by Raman spectroscopy. The Raman spectra revealed inherent spectral markers for the opaque, capsule-positive strain AB5075 (and AB5075::lux), specifically the Raman spectral bands at 979 $cm^{-1}$ (A) and 1,422 $cm^{-1}$ and 1,379 $cm^{-1}$ (B). These spectral bands were absent in the capsule-negative strains AB5075P, AB5075 *epsA*::Tn*5*, AB5075 *ptk*::Tn*5*, and streak-purified AB-Army1-treated AB5075 (and AB5075::lux). a.u., arbitrary units.

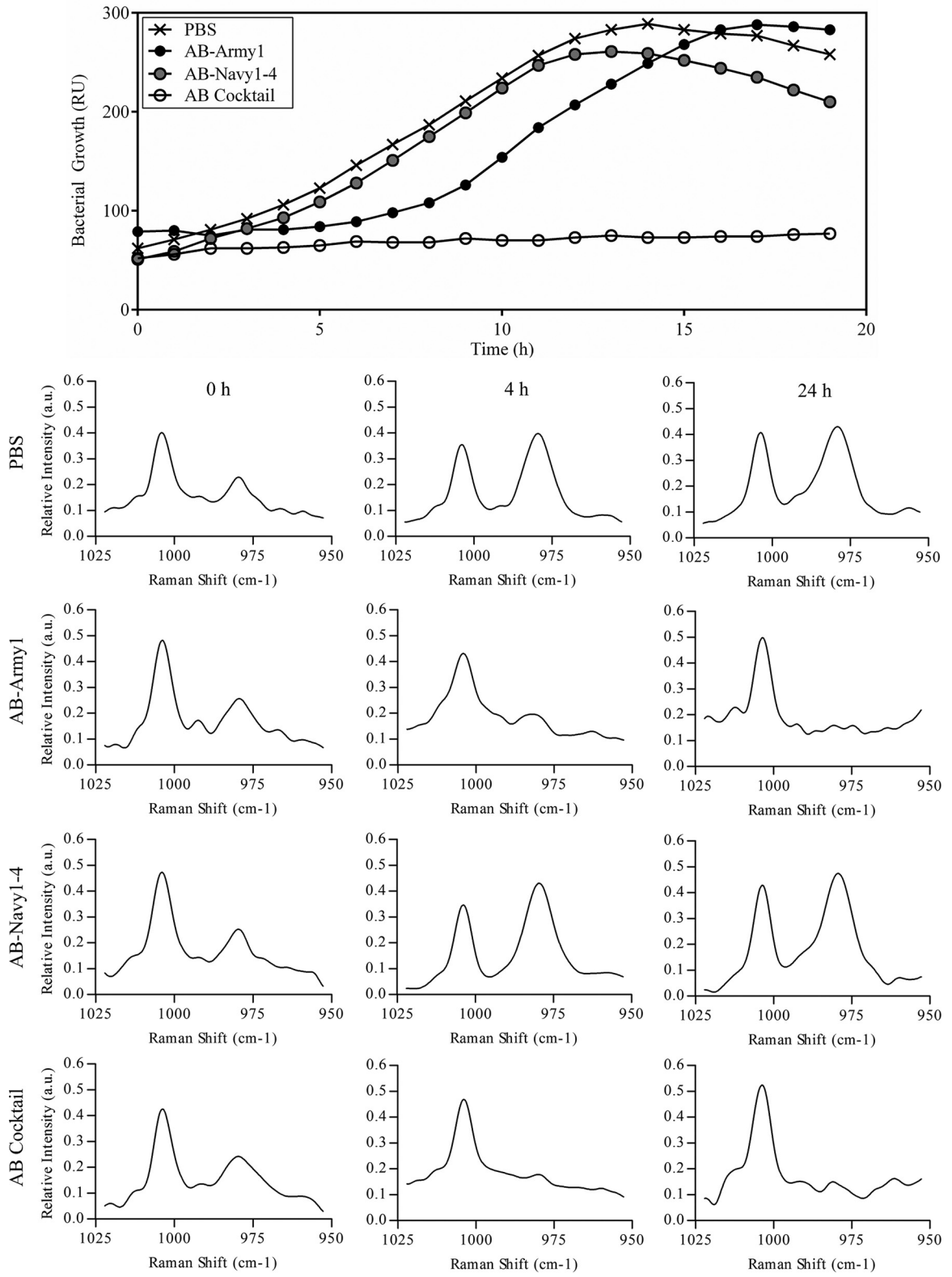


**FIG 3** Infection of AB5075 with the five-member AB cocktail results in complete killing *in vitro*. (Top panel) AB5075 was grown in the Biolog system for 19 h in the presence of AB-Army1, AB-Navy1–4, or the AB cocktail. Treatment with AB-Navy1–4 resulted in no change in growth compared to that of PBS-treated cells. AB-Army1 infection resulted in an extended lag phase, due to the 99% killing of capsule-positive cells, and the eventual outgrowth of capsule-negative cells. RU, relative units. (Bottom panels) Raman spectra were collected on samples at 0, 4, and 24 h. For AB5075 treated with AB-Army1 or the AB cocktail, the 979 $cm^{-1}$ band decreased over the course of the experiment.

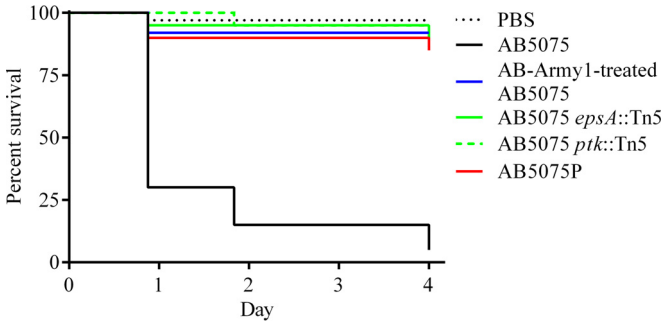


**FIG 4** Translucent, capsule-negative strains are attenuated in a *Galleria mellonella* model. Kaplan-Meier survival curves of *G. mellonella* worms infected with $5 \times 10^4$ CFU of capsulated wild-type AB5075 or uncapsulated AB5075 strains. Curves were compared using the Mantel-Cox test with Bonferroni's correction for multiple comparisons. Capsulated AB5075 displayed significantly increased mortality in comparison to the other strains ($P < 0.0006$).

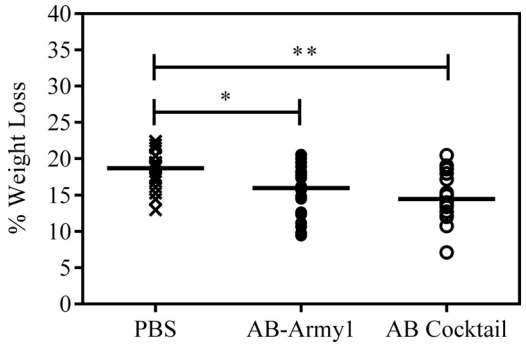


**FIG 5** Change in mouse weight on day 2 postinfection. On day 2, the median weight losses were 18.7%, 16.0%, and 14.5% for PBS-, AB-Army1-, and AB cocktail-treated mice, respectively. Statistical analysis using a Kruskal-Wallis test, followed by Dunn's multiple-comparison test, found a significant difference between control and cocktail-treated mice ($P \leq 0.01$) and control and monophage-treated mice ($P \leq 0.05$). Figure S1 in the supplemental material shows all weights for days 1 to 5 postinfection.

Again using the Biolog system, it was determined that the AB cocktail infected 10 out of the 92 strains (see Table S1 in the supplemental material), highlighting the specificity of the cocktail and thus the probable need for personalization when using phages therapeutically.

**The virulence of AB-Army1-treated AB5075 is attenuated in a *Galleria mellonella* model.** AB5075 bacteria previously exposed to AB-Army1 phage displayed a translucent phenotype similar to that of *epsA* and *ptk* capsule mutants. Because *A. baumannii epsA* and *ptk* mutants have been shown to be attenuated in an animal model (34), we hypothesized that translucent AB5075 bacteria previously exposed to AB-Army1 phage would be less virulent than wild-type AB5075 bacteria in a *G. mellonella* wax worm model of infection (35, 49). Evaluation of AB5075, AB-Army1-exposed AB5075, AB5075P, AB5075 *epsA*::Tn*5*, and AB5075 *ptk*::Tn*5* in the worm model confirmed that all four translucent strains were avirulent in comparison to capsule-positive AB5075 (Fig. 4). After day 4 postinfection, the survival rate of worms infected with AB5075 was 5%, while all other groups had survival rates of 85% or greater. Analysis of these curves using a Mantel-Cox test with Bonferroni's correction for multiple comparisons determined that the difference was statistically significant ($P < 0.0006$). During the experiment, one of the PBS control worms died, likely due to injection trauma from the route of infection. A control group of untouched worms had 100% survival during the course of the experiment.

**Treatment of AB5075-infected wounds with the AB cocktail leads to vastly improved clinical outcomes in a mouse wound model.** We wanted to determine if the bactericidal activity of the AB cocktail observed *in vitro* could be recapitulated in a mouse wound model and result in an effective treatment against AB5075-infected wounds. Briefly, neutropenic mice were subjected to a full-thickness dorsal wound via a 6-mm biopsy punch, and the wound was infected with MDR *A. baumannii* AB5075::lux, a bioluminescent isogenic strain of AB5075 (see Materials and Methods). The measured outcomes for the wound experiments included (i) surgery/infection-associated weight loss, (ii) average radiance of bioluminescent bacteria in the wound bed, (iii) area of the infection as monitored by the area of bioluminescence, (iv) physical wound size, and (v) biofilm formation on wound dressings.

Infection-associated weight loss is an established measure of morbidity in mice (30). The body weight of each animal was measured through day 5 of the infection, and the percent weight loss was calculated in comparison to day 0. The peak weight loss occurred on day 2, and the mice began to gain weight on day 3 (see Fig. S1 in the supplemental material). On day 2, the median weight losses were 18.7%, 16.0%, and 14.5% for PBS-, AB-Army1-, and AB cocktail-treated mice, respectively (Fig. 5). Statistical analysis using a Kruskal-Wallis test followed by Dunn's multiple-comparison test found significant differences between PBS- and AB cocktail-treated mice ($P \leq 0.01$) and between PBS- and AB-Army1-treated mice ($P \leq 0.05$). Thus, mice receiving either phage treatment lost less weight than the PBS-treated group during the infection and recovery.

During the course of the infection, the wounds were monitored for bioburden as a function of average radiance and area of bioluminescence using an IVIS *in vivo* imaging system. Bioluminescence was measured on days 1, 3, and 5 postinfection. After day 5, the bioluminescence was below background levels for all treatment groups. Heat maps of the wound bioburden suggested a difference in both signal intensity and area of infection among the groups; the most evident difference was seen on day 5, when the AB cocktail-treated wound displayed no signal (Fig. 6; see Fig. S2 in the supplemental material). When bioluminescence was quantified, the AB cocktail-treated mice had significantly less bioluminescence than the PBS- or AB-Army1-treated mice throughout the experiment, indicative of a reduced bacterial burden in the AB cocktail-treated mice with respect to the other treatment groups ($P \leq 0.01$) (Fig. 7). The area of the bioluminescence was also measured to evaluate how far the *A. baumannii* AB5075::lux bacteria disseminated into tissue surrounding the surgical wound bed. For each day measured, the area of bioluminescence in the AB cocktail-treated wounds was significantly smaller than that of PBS-treated wounds ($P \leq 0.05$) (Fig. 8), suggesting that this treatment prevented the dissemination of AB5075::lux bacteria into the surrounding tissue. Thus, both the bioburden and the infection area, as monitored by bioluminescence, were significantly reduced in the mice treated with the five-member phage cocktail throughout the infection.

Previous studies have shown that the proliferation of bacte-

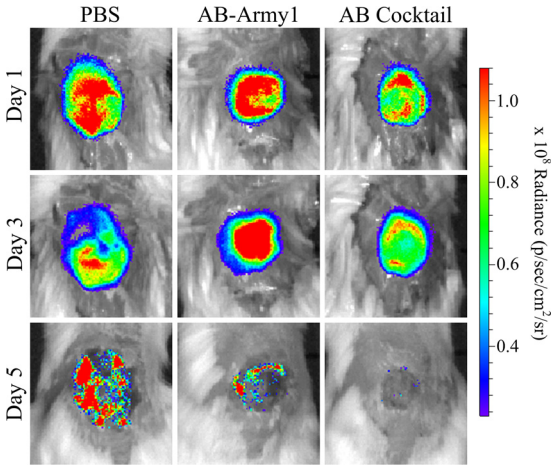


**FIG 6** Bioluminescence of the infected wound bed. The bioluminescence of *A. baumannii* AB5075::lux was measured (in photons/s/cm$^2$/steradian) for each mouse wound by using an IVIS *in vivo* imaging system. Pictured are exemplar images of wound bioluminescence of mice from each group on days 1, 3, and 5 postinfection. Figure S2 in the supplemental material shows all IVIS images for every mouse used in this study.

ria outside the initial boundaries of the surgical wound results in necrosis of the surrounding tissue and an increase in wound size over the course of the experiment (30). In agreement with these observations, the area of bioluminescence measured here was consistent with the physical wound size, as measured using the Aranz Silhouette system (Fig. 9A). On day 9, there were significant differences in median wound size between the PBS and AB cocktail ($P \leq 0.001$) groups and between the PBS and AB-Army1 ($P \leq 0.01$) groups. A similar trend was also observed on day 13 between the PBS and AB cocktail ($P \leq 0.001$) groups and the AB-Army1 and AB cocktail ($P \leq 0.001$) groups. Thus, on days 9 and 13, the AB cocktail-treated group had significantly smaller wounds.

Additionally, median wound sizes were compared within each group across days (Fig. 9B). During the course of the experiment, maximum wound size was reached on day 9 and

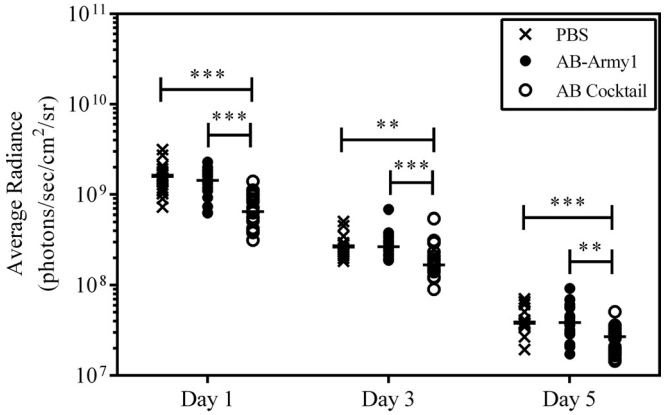


**FIG 7** Bioluminescence of *A. baumannii* AB5075::lux in the mouse wound. The photon emission of each wound was measured (in photons/s/cm$^2$/steradian) using an IVIS *in vivo* imaging system on days 1, 3, and 5 postinfection. Statistical analysis was completed using a Kruskal-Wallis test, followed by Dunn's multiple-comparison test. **, $P \leq 0.01$; ***, $P \leq 0.001$.

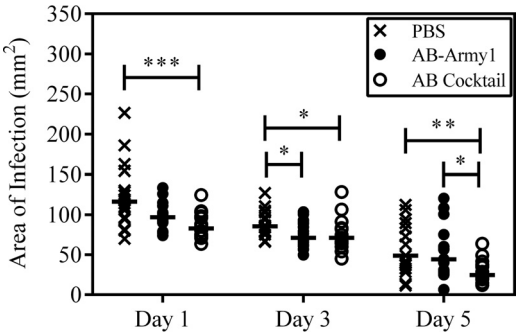


**FIG 8** Infection area of *A. baumannii* AB5075::lux in the mouse wound. The area of bioluminescence of *A. baumannii* was measured to evaluate the dispersal of AB5075::lux bacteria to areas outside the initial boundaries of the surgical wound. Statistical analysis was completed using a Kruskal-Wallis test, followed by Dunn's multiple-comparison test. *, $P \leq 0.05$; **, $P \leq 0.01$; ***, $P \leq 0.001$.

then the wounds began to heal and contract. In the PBS-treated mice, there was a significant increase in wound size between days 3 and 9 ($P \leq 0.001$). Less drastic but significant increases were also seen in the AB-Army1-treated mice between days 3 and 9 ($P \leq 0.05$). Conversely, there was no statistical difference in wound size for the AB cocktail group between days 3 and 9, further suggesting that the five-member cocktail treatment prevented bacterial dissemination and tissue necrosis outside

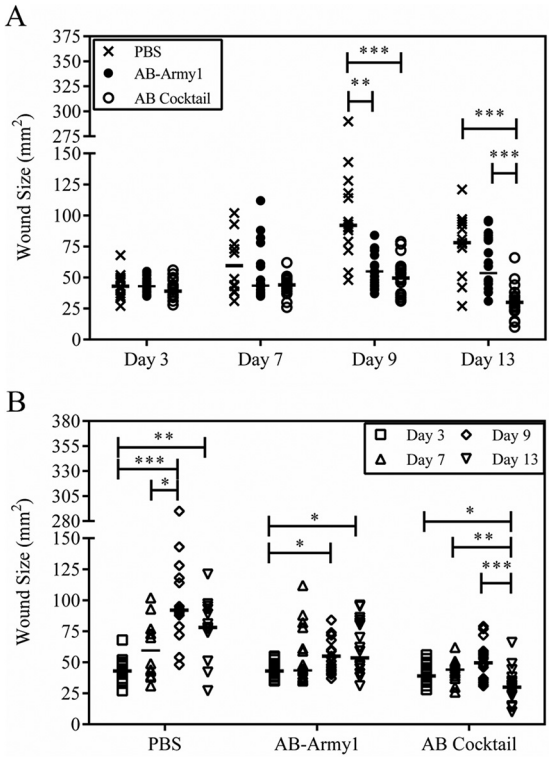


**FIG 9** Size of mouse wounds over the course of infection. The size of each mouse wound was measured using the Aranz Silhouette system on days 3, 7, 9, and 13 postinfection. (A) Comparison of treatments on days 3, 7, 9, and 13. (B) Comparison within each treatment group across days 3, 7, 9, and 13. Statistical analysis was completed using a Kruskal-Wallis test, followed by Dunn's multiple-comparison test. *, $P \leq 0.05$; **, $P \leq 0.01$; ***, $P \leq 0.001$.

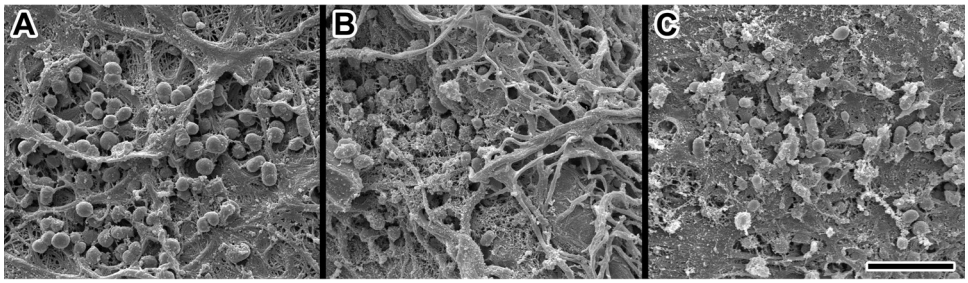


**FIG 10** Scanning electron micrographs of *A. baumannii* AB5075::lux on Tegaderm bandages. Bacteria are associated with fibroblast products and other components of the wound surface after Tegaderm bandage removal from the wound site. (A) PBS-treated mouse; (B) AB-Army1-treated mouse; (C) AB cocktail-treated mouse. Scale bar, 4 μm.

the original surgical wound bed and as a result the wounds never increased in size. It is important to note that there was a statistically significant difference in wound size for the AB cocktail-treated mice on day 13, compared to that on days 3, 7, and 9. However, this difference was due to a decrease in wound size on day 13 as a result of healing (Fig. 9B).

Tegaderm dressings that were removed on day 3 postinfection from each group of mice were fixed and visualized by SEM to determine if phage treatment affected the ability of *A. baumannii* AB5075::lux to form biofilm on the bandage. A robust biofilm formed on the Tegaderm dressings in the PBS- and AB-Army1-treated mice, as visualized by a complex exopolysaccharide structure; however, very little mature biofilm structure was present on the Tegaderm dressings from the AB cocktail-treated mice (Fig. 10).

It is important to note that during the animal experiment, there were a total of three deaths occurring on days 2 and 3 in the PBS control group. There were also two mice that had to be euthanized due to hind limb paralysis on days 4 and 5 in the PBS control group. In addition, all of the mice in the PBS control group displayed additional clinical signs of illness, including conjunctivitis, ruffled fur from reduced grooming, and decreased mobility. These kinds of negative outcomes were never observed in either of the phage treatment groups.

## DISCUSSION

The prevalence of MDR bacterial pathogens is a growing threat to public health, and it is increasingly obvious that new treatment options are needed. Bacteriophages have reemerged as candidates for new, targeted antibacterial therapeutics. In this work, we successfully isolated and purified several wild environmental phages against *A. baumannii* and demonstrated that these phages can be rapidly compounded into a cocktail that successfully treats *A. baumannii* wound infections in mice. The isolation and purification of these phages from local sewage water show that phages with lytic activity against a clinically relevant pathogen can be easily and rapidly purified from environmental sources. It should be noted that the *A. baumannii* isolates used for phage isolation were not cured of any potential prophages first, as is customary when propagating phages in a laboratory setting. Although contaminating lysogens may be present in our phage preparations, the lytic activity of the therapeutic phages is not hindered, as we still see lysis *in vitro* and efficacy *in vivo*. In addition, any personalized cocktail for a clinical isolate could have unknown prophages as well, and taking time to cure prophages from these strains would prevent rapid personalized phage cocktail formulation, which we propose is the most viable path forward for phage therapeutic development.

Using these phages in the five-member AB cocktail, we demonstrated effective killing of AB5075 bacteria *in vitro* and showed that the observed bactericidal activity occurs in a synergistic manner. AB-Army1 imposes a strong selection for the loss of receptor, likely a capsule component, and the resulting emergent uncapsulated cells were then sensitized to the AB-Navy1–4 phages. When testing the AB cocktail against a collection of 92 MDR *A. baumannii* clinical isolates, we found that only 10 of the strains were successfully infected, highlighting the narrow spectrum of phages and the need for personalization when developing phages as a therapeutic against MDR infections.

In agreement with our *in vitro* findings, a similar bactericidal effect was also observed when the AB cocktail was used as a therapeutic against AB5075::lux-infected wounds in mice. Compared to PBS-treated controls, mice treated with the five-member AB cocktail had reductions in weight loss, wound bioburden, area of infection, and wound size throughout the course of the study. A lack of biofilm observed on Tegaderm dressings of AB cocktail-treated mice also suggests that phage treatment prevents biofilm formation, and this specific mode of action may play a role in preventing the dissemination of bacteria into the surrounding tissue. The AB cocktail-treated group also had no fatalities or paralysis events. By every metric followed here, the personalized phage cocktail we developed serves as an effective treatment against MDR *A. baumannii* AB5075 wound infections in this model (30). While the individual AB-Army1 phage did show some efficacy, it was not as effective as the full AB cocktail, consistent with the combinatorial effect seen *in vitro*. It should be noted that we administered a high dose of phage both topically and systemically here, at 4 h postinfection. While it is known that at 4 h postinfection, the number of *A. baumannii* AB5075 CFU increased by at least 1 log in the mouse wound model (30), work is ongoing to determine if these phages can be effective against a more established infection and if a single route of administration at a lower dose would produce similar outcomes.

Phages are narrow spectrum even to the subspecies level, which is of value when trying to avoid damage to the host microbiome but poses a significant challenge when developing a therapeutic to be used widely to treat infection. Thus, it is likely that phages will be most viable as a personalized therapeutic, where a specific bacterial isolate from a patient is used to produce a customized cocktail that is rapidly compounded to treat that specific patient and infection. Here we demon-

strate that wild, environmental phages can be easily purified and rapidly compounded against the MDR clinical isolate AB5075 using a high-throughput liquid assay. In the future, it may be advantageous to use a large sequenced library of pathogen-specific down-selected phages, so as to eliminate phages harboring toxins and known lysogeny genes, etc. Importantly, knowing the precise receptor for each phage in such a library may not be needed. Based on our results here, the presumed receptor of the AB-Army1 phage is a component of the capsule, a known virulence factor of *A. baumannii* (33, 34). However, identifying the precise receptor was not required to determine that AB-Army1 infection appears to impose a strong selection for AB5075 cells that display a phenotype consistent with loss of capsule and are avirulent in the *G. mellonella* survival model. In addition, receptor identification was not required to observe the synergistic killing of AB5075 by the full AB cocktail. Synergistic killing can be observed empirically apart from a mechanistic understanding of the receptor. Receptor identification is a nontrivial task and would hinder the rapid formulation of cocktails in a personalized manner. Instead, we argue that it is simply necessary to use diverse phages with distinct but overlapping host ranges that show synergistic killing in a liquid-based assay. The efficacy of such a synergistic cocktail is most likely due to those phages having different receptors; however, knowing their identities is not critical to therapeutic performance. Thus, by beginning with a diverse library of known and sequenced phages, cocktails could be rapidly compounded based simply on performance.

Personalized phage cocktail formulation in a clinically relevant time frame from a known library may require new diagnostic techniques to assist screening phage libraries. Here, Raman spectroscopy could distinguish between strains susceptible to AB-Army1 and those that are resistant. Because of the speed of Raman spectroscopy and the lack of a requirement for culturing, we are pursuing the use of Raman spectroscopy to assist in rapid cocktail formulation.

Phage cocktails represent a new class of therapeutic that is completely dissimilar to small-molecule antibiotics, in both their mechanisms of action and how they are produced. In order to effectively transition a phage therapeutic for human use, there will likely need to be a new regulatory framework that governs natural phage-based products specifically. We believe that this is essential in order to develop novel, efficacious therapies against the MDR ESKAPE pathogens.

## ACKNOWLEDGMENTS

The work presented here was funded through the Military Infectious Disease Research Program (W0121_14_NM) and supported by work unit number A1416. R. M. Hannah was funded under agreement no. HSHQDC-07-C-00020, which was awarded by the U.S. Department of Homeland Security (DHS) for the management and operation of the National Biodefense Analysis and Countermeasures Center (NBACC), a federally funded research and development center.

We kindly acknowledge the WRAIR Wound Infections animal team for their assistance in carrying out the mouse wound model studies. We thank Robert Pope for his advice on electron microscopy.

The views expressed in this article are those of the authors and do not necessarily reflect the official policies or positions of the Department of the Navy, the Department of the Army, the Department of Defense, or the U.S. Government. The material has been reviewed by the Walter Reed Army Institute of Research, and there is no objection to its presentation and/or publication.

## FUNDING INFORMATION

This work, including the efforts of James M. Regeimbal, Matthew S. Henry, Rebecca L. Pavlicek, Javier Quinones, Nimfa C. Teneza-Mora, Biswajit Biswas, and Eric R. Hall, was funded by Military Infectious Disease Research Program (W0121_14_NM). This work, including the efforts of Ryan M. Hannah, was funded by U.S. Department of Homeland Security (DHS) (HSHQDC-07-C-00020).

The funders had no role in study design, data collection and interpretation, or the decision to submit the work for publication.

## REFERENCES

1. **Boucher HW, Talbot GH, Bradley JS, Edwards JE, Gilbert D, Rice LB, Scheld M, Spellberg B, Bartlett J.** 2009. Bad bugs, no drugs: no ESKAPE! An update from the Infectious Diseases Society of America. Clin Infect Dis **48:**1–12. http://dx.doi.org/10.1086/595011.
2. **Pendleton JN, Gorman SP, Gilmore BF.** 2013. Clinical relevance of the ESKAPE pathogens. Expert Rev Anti Infect Ther **11:**297–308. http://dx.doi.org/10.1586/eri.13.12.
3. **Murray CK, Hospenthal DR.** 2008. Acinetobacter infection in the ICU. Crit Care Clin **24:**237–248, vii. http://dx.doi.org/10.1016/j.ccc.2007.12.005.
4. **Calhoun JH, Murray CK, Manring MM.** 2008. Multidrug-resistant organisms in military wounds from Iraq and Afghanistan. Clin Orthop Relat Res **466:**1356–1362. http://dx.doi.org/10.1007/s11999-008-0212-9.
5. **Crane DP, Gromov K, Li D, Soballe K, Wahnes C, Buchner H, Hilton MJ, O'Keefe RJ, Murray CK, Schwarz EM.** 2009. Efficacy of colistin-impregnated beads to prevent multidrug-resistant A. baumannii implant-associated osteomyelitis. J Orthop Res **27:**1008–1015. http://dx.doi.org/10.1002/jor.20847.
6. **DeLeon K, Balldin F, Watters C, Hamood A, Griswold J, Sreedharan S, Rumbaugh KP.** 2009. Gallium maltolate treatment eradicates Pseudomonas aeruginosa infection in thermally injured mice. Antimicrob Agents Chemother **53:**1331–1337. http://dx.doi.org/10.1128/AAC.01330-08.
7. **Griffith ME, Lazarus DR, Mann PB, Boger JA, Hospenthal DR, Murray CK.** 2007. Acinetobacter skin carriage among US army soldiers deployed in Iraq. Infect Control Hosp Epidemiol **28:**720–722. http://dx.doi.org/10.1086/518966.
8. **Hawley JS, Murray CK, Griffith ME, McElmeel ML, Fulcher LC, Hospenthal DR, Jorgensen JH.** 2007. Susceptibility of Acinetobacter strains isolated from deployed U.S. military personnel. Antimicrob Agents Chemother **51:**376–378. http://dx.doi.org/10.1128/AAC.00858-06.
9. **Hawley JS, Murray CK, Jorgensen JH.** 2007. Development of colistin-dependent Acinetobacter baumannii-Acinetobacter calcoaceticus complex. Antimicrob Agents Chemother **51:**4529–4530. http://dx.doi.org/10.1128/AAC.01115-07.
10. **Hawley JS, Murray CK, Jorgensen JH.** 2008. Colistin heteroresistance in Acinetobacter and its association with previous colistin therapy. Antimicrob Agents Chemother **52:**351–352. http://dx.doi.org/10.1128/AAC.00766-07.
11. **Hujer KM, Hujer AM, Hulten EA, Bajaksouzian S, Adams JM, Donskey CJ, Ecker DJ, Massire C, Eshoo MW, Sampath R, Thomson JM, Rather PN, Craft DW, Fishbain JT, Ewell AJ, Jacobs MR, Paterson DL, Bonomo RA.** 2006. Analysis of antibiotic resistance genes in multidrug-resistant Acinetobacter sp. isolates from military and civilian patients treated at the Walter Reed Army Medical Center. Antimicrob Agents Chemother **50:**4114–4123. http://dx.doi.org/10.1128/AAC.00778-06.
12. **Michalopoulos A, Falagas ME.** 2010. Treatment of Acinetobacter infections. Expert Opin Pharmacother **11:**779–788. http://dx.doi.org/10.1517/14656561003596350.
13. **Tribble DR, Conger NG, Fraser S, Gleeson TD, Wilkins K, Antonille T, Weintrob A, Ganesan A, Gaskins LJ, Li P, Grandits G, Landrum ML, Hospenthal DR, Millar EV, Blackbourne LH, Dunne JR, Craft D, Mende K, Wortmann GW, Herlihy R, McDonald J, Murray CK.** 2011. Infection-associated clinical outcomes in hospitalized medical evacuees after traumatic injury: trauma infectious disease outcome study. J Trauma **71:**S33–S42. http://dx.doi.org/10.1097/TA.0b013e318221162e.
14. **Yun HC, Branstetter JG, Murray CK.** 2008. Osteomyelitis in military personnel wounded in Iraq and Afghanistan. J Trauma **64:**S163–S168; discussion S168. http://dx.doi.org/10.1097/TA.0b013e318160868c.
15. **d'Herelle F.** 1917. An invisible antagonist microbe of dysentery bacillus. Compte Rendus Hebdomadaires Seances Acad Sci **165:**373–375.

16. **Eaton MD, Bayne-Jones S.** 1934. Bacteriophage therapy. JAMA **103:** 1769–1776, 1847–1853, 1934–1939. http://dx.doi.org/10.1001/jama.1934.72750490003007.
17. **Marcuk LM, Nikiforov VN, Scerbak JF, Levitov TA, Kotljarova RI, Naumsina MS, Davydov SU, Monsur KA, Rahman MA, Latif MA, Northrup RS, Cash RA, Hug I, Dey CR, Phillips RA.** 1971. Clinical studies of the use of bacteriophage in the treatment of cholera. Bull World Health Organ **45:**77–83.
18. **Smith HW, Huggins MB.** 1982. Successful treatment of experimental Escherichia coli infections in mice using phage: its general superiority over antibiotics. J Gen Microbiol **128:**307–318.
19. **Soothill JS.** 1992. Treatment of experimental infections of mice with bacteriophages. J Med Microbiol **37:**258–261. http://dx.doi.org/10.1099/00222615-37-4-258.
20. **Merril CR, Biswas B, Carlton R, Jensen NC, Creed GJ, Zullo S, Adhya S.** 1996. Long-circulating bacteriophage as antibacterial agents. Proc Natl Acad Sci U S A **93:**3188–3192. http://dx.doi.org/10.1073/pnas.93.8.3188.
21. **Alisky J, Iczkowski K, Rapoport A, Troitsky N.** 1998. Bacteriophages show promise as antimicrobial agents. J Infect **36:**5–15. http://dx.doi.org/10.1016/S0163-4453(98)92874-2.
22. **Biswas B, Adhya S, Washart P, Paul B, Trostel AN, Powell B, Carlton R, Merril CR.** 2002. Bacteriophage therapy rescues mice bacteremic from a clinical isolate of vancomycin-resistant Enterococcus faecium. Infect Immun **70:**204–210. http://dx.doi.org/10.1128/IAI.70.1.204-210.2002.
23. **Merril CR, Scholl D, Adhya SL.** 2003. The prospect for bacteriophage therapy in Western medicine. Nat Rev Drug Discov **2:**489–497. http://dx.doi.org/10.1038/nrd1111.
24. **Bruttin A, Brussow H.** 2005. Human volunteers receiving Escherichia coli phage T4 orally: a safety test of phage therapy. Antimicrob Agents Chemother **49:**2874–2878. http://dx.doi.org/10.1128/AAC.49.7.2874-2878.2005.
25. **Rhoads DD, Wolcott RD, Kuskowski MA, Wolcott BM, Ward LS, Sulakvelidze A.** 2009. Bacteriophage therapy of venous leg ulcers in humans: results of a phase I safety trial. J Wound Care **18:**237–238, 240–233. http://dx.doi.org/10.12968/jowc.2009.18.6.42801.
26. **Kutter E, De Vos D, Gvasalia G, Alavidze Z, Gogokhia L, Kuhl S, Abedon ST.** 2010. Phage therapy in clinical practice: treatment of human infections. Curr Pharm Biotechnol **11:**69–86. http://dx.doi.org/10.2174/138920110790725401.
27. **Chan BK, Abedon ST, Loc-Carrillo C.** 2013. Phage cocktails and the future of phage therapy. Future Microbiol **8:**769–783. http://dx.doi.org/10.2217/fmb.13.47.
28. **Sambrook J, Fritsch EF, Maniatis T.** 1989. Molecular cloning: a laboratory manual, 2nd ed. Cold Spring Harbor Press, Cold Spring Harbor, NY.
29. **Jacobs AC, Thompson MG, Black CC, Kessler JL, Clark LP, McQueary CN, Gancz HY, Corey BW, Moon JK, Si Y, Owen MT, Hallock JD, Kwak YI, Summers A, Li CZ, Rasko DA, Penwell WF, Honnold CL, Wise MC, Waterman PE, Lesho EP, Stewart RL, Actis LA, Palys TJ, Craft DW, Zurawski DV.** 2014. AB5075, a highly virulent isolate of Acinetobacter baumannii, as a model strain for the evaluation of pathogenesis and antimicrobial treatments. mBio **5:**e01076-14. http://dx.doi.org/10.1128/mBio.01076-14.
30. **Thompson MG, Black CC, Pavlicek RL, Honnold CL, Wise MC, Alamneh YA, Moon JK, Kessler JL, Si Y, Williams R, Yildirim S, Kirkup BC, Jr, Green RK, Hall ER, Palys TJ, Zurawski DV.** 2014. Validation of a novel murine wound model of Acinetobacter baumannii infection. Antimicrob Agents Chemother **58:**1332–1342. http://dx.doi.org/10.1128/AAC.01944-13.
31. **Kumar A, Dalton C, Cortez-Cordova J, Schweizer HP.** 2010. Mini-Tn7 vectors as genetic tools for single copy gene cloning in Acinetobacter baumannii. J Microbiol Methods **82:**296–300. http://dx.doi.org/10.1016/j.mimet.2010.07.002.
32. **Henry M, Biswas B, Vincent L, Mokashi V, Schuch R, Bishop-Lilly KA, Sozhamannan S.** 2012. Development of a high throughput assay for indirectly measuring phage growth using the OmniLog™ system. Bacteriophage **2:**159–167. http://dx.doi.org/10.4161/bact.21440.
33. **Luke NR, Sauberan SL, Russo TA, Beanan JM, Olson R, Loehfelm TW, Cox AD, St Michael F, Vinogradov EV, Campagnari AA.** 2010. Identification and characterization of a glycosyltransferase involved in *Acinetobacter baumannii* lipopolysaccharide core biosynthesis. Infect Immun **78:**2017–2023. http://dx.doi.org/10.1128/IAI.00016-10.
34. **Russo TA, Luke NR, Beanan JM, Olson R, Sauberan SL, Macdonald U, Schultz LW, Umland TC, Campagnari AA.** 2010. The K1 capsular polysaccharide of *Acinetobacter baumannii* 307-0294 is a major virulence factor. Infect Immun. **78:**3993–4000. http://dx.doi.org/10.1128/IAI.00366-10.
35. **Peleg AY, Jara S, Monga D, Eliopoulos GM, Moellering RC, Jr, Mylonakis E.** 2009. Galleria mellonella as a model system to study Acinetobacter baumannii pathogenesis and therapeutics. Antimicrob Agents Chemother **53:**2605–2609. http://dx.doi.org/10.1128/AAC.01533-08.
36. **National Research Council.** 2011. Guide for the care and use of laboratory animals, 8th ed. National Academies Press, Washington, DC.
37. **Azeredo J, Sutherland IW.** 2008. The use of phages for the removal of infectious biofilms. Curr Pharm Biotechnol **9:**261–266. http://dx.doi.org/10.2174/138920108785161604.
38. **Bessler W, Fehmel F, Freund-Molbert E, Knufermann H, Stirm S.** 1975. Escherichia coli capsule bacteriophages. IV. Free capsule depolymerase 29. J Virol **15:**976–984.
39. **Cornelissen A, Ceyssens PJ, T'Syen J, Van Praet H, Noben JP, Shaburova OV, Krylov VN, Volckaert G, Lavigne R.** 2011. The T7-related Pseudomonas putida phage phi15 displays virion-associated biofilm degradation properties. PLoS One **6:**e18597. http://dx.doi.org/10.1371/journal.pone.0018597.
40. **Hughes KA, Sutherland IW, Clark J, Jones MV.** 1998. Bacteriophage and associated polysaccharide depolymerases—novel tools for study of bacterial biofilms. J Appl Microbiol **85:**583–590. http://dx.doi.org/10.1046/j.1365-2672.1998.853541.x.
41. **Hughes KA, Sutherland IW, Jones MV.** 1998. Biofilm susceptibility to bacteriophage attack: the role of phage-borne polysaccharide depolymerase. Microbiology **144:**3039–3047. http://dx.doi.org/10.1099/00221287-144-11-3039.
42. **Kassa T, Chhibber S.** 2012. Thermal treatment of the bacteriophage lysate of Klebsiella pneumoniae B5055 as a step for the purification of capsular depolymerase enzyme. J Virol Methods **179:**135–141. http://dx.doi.org/10.1016/j.jviromet.2011.10.011.
43. **Sutherland IW.** 1995. Polysaccharide lyases. FEMS Microbiol Rev **16:**323–347. http://dx.doi.org/10.1111/j.1574-6976.1995.tb00179.x.
44. **Linnerborg M, Weintraub A, Albert MJ, Widmalm G.** 2001. Depolymerization of the capsular polysaccharide from Vibrio cholerae O139 by a lyase associated with the bacteriophage JA1. Carbohydr Res **333:**263–269. http://dx.doi.org/10.1016/S0008-6215(01)00159-8.
45. **Tipton KA, Dimitrova D, Rather PN.** 2015. Phase-variable control of multiple phenotypes in Acinetobacter baumannii strain AB5075. J Bacteriol **197:**2593–2599. http://dx.doi.org/10.1128/JB.00188-15.
46. **Senchenkova SN, Shashkov AS, Popova AV, Shneider MM, Arbatsky NP, Miroshnikov KA, Volozhantsev NV, Knirel YA.** 2015. Structure elucidation of the capsular polysaccharide of Acinetobacter baumannii AB5075 having the KL25 capsule biosynthesis locus. Carbohydr Res **408:**8–11. http://dx.doi.org/10.1016/j.carres.2015.02.011.
47. **Naumann D.** 2001. FT-infrared and FT-Raman spectroscopy in biomedical research, p 329–337. *In* Gremlich HU, Yan B (ed), Infrared and Raman spectroscopy of biological materials. CRC Press, New York, NY.
48. **Socrates G.** 2004. Infrared and Raman characteristic group frequencies: tables and charts, 3rd ed. John Wiley & Sons, Ltd, New York, NY.
49. **Loh JM, Adenwalla N, Wiles S, Proft T.** 2013. Galleria mellonella larvae as an infection model for group A streptococcus. Virulence **4:**419–428. http://dx.doi.org/10.4161/viru.24930.